The Phenotypic Spectrum of Sporadic Creutzfeldt-Jakob Disease Cortical Subtype

Simone Baiardi, MD, PhD,[1,2] Claudia Marina Vargiu, MSc,[2] Brian S. Appleby, MD,[3,4,5] Marcelo Barria, PhD,[6] Giuseppe Mario Bentivenga, MD,[1] Ignazio Calì, PhD,[3,4] Benedetta Carlà, MSc,[2] Mark Cohen, MD,[3,4] Armin Giese, MD,[7] Jochen Herms, MD,[7,8] Aino-Minerva Kortelainen, MD,[6] Anna Ladogana, MD,[9] Angela Mammana, PhD,[2] Diane Ritchie, MD,[6] Otto Windl, PhD,[7] Sabina Capellari, MD,[1,2] and Piero Parchi, MD, PhD[1,2]

Objective: The objective of this study was to characterize the phenotypic spectrum of the rare sporadic Creutzfeldt-Jakob disease cortical subtype (sCJDMM/MV2C) in a large multicentric autopsy cohort.
Methods: We evaluated clinical histories, biofluid markers, brain diffusion-weighted (DW)-magnetic resonance imaging (MRI), and electroencephalogram (EEG) findings in 56 patients. The histomolecular assessment included misfolded prion protein (PrP) typing by immunoblotting, histopathology, and PrP immunohistochemistry in several brain areas.
Results: Misfolded PrP typing showed a dominant 19 kDa unglycosylated PrP fragment (type 2) in all brains, focally associated with a 21 kDa (type 1) fragment in 53% of participants (MM/MV2C + 1). Immunohistochemistry revealed coarse/perivacuolar PrP deposits in the neocortices and a patchy/coarse pattern in the cerebellar molecular layer. The mean disease duration was 16.0 months. At onset and early stages, most patients manifested only progressive cognitive decline, consistent with the predominant distribution and relative severity of spongiform change in the cerebral cortex. Brain DW-MRI showed cortical hyperintensities in 94% of cases. Cerebrospinal fluid (CSF) real-time quaking-induced conversion (RT-QuIC) assay was positive in 70% of cases. Compared with pure MM/MV2C, the mixed MM/MV2C + 1 phenotype showed a shorter disease duration (14 vs 19 months), and a higher frequency of striatal DW-MRI hyperintensity (56% vs 19%), EEG periodic sharp-waves complexes (41% vs 6%), and CSF RT-QuIC positivity (86% vs 53%).
Interpretation: The clinicopathologic phenotype of sCJDMM/MV2C diverges from that of typical sCJDMM/MV1. Moreover, the histomolecular heterogeneity within MM/MV2C influences clinical features and results of diagnostic investigations, challenging its identification in vivo. Nonetheless, results suggest that DW-MRI and CSF RT-QuIC allow an accurate clinical diagnosis of Creutzfeldt-Jakob disease in most patients.

ANN NEUROL 2025;00:1–14

View this article online at wileyonlinelibrary.com. DOI: 10.1002/ana.78117

Received Aug 27, 2025, and in revised form Oct 28, 2025. Accepted for publication Dec 1, 2025.

Address correspondence to Dr Piero Parchi, IRCCS Istituto delle Scienze Neurologiche, Ospedale Bellaria, Via Altura 1/8, 40139 Bologna, Italy.
E-mail: piero.parchi@unibo.it
Current address for Armin Giese: MODAG GmbH, Wendelsheim, Germany

From the [1]Department of Biomedical and Neuromotor Sciences (DIBINEM), University of Bologna, Bologna, Italy; [2]IRCCS Istituto delle Scienze Neurologiche di Bologna, Bologna, Italy; [3]Department of Pathology, School of Medicine, Case Western Reserve University, Cleveland, OH; [4]National Prion Disease Pathology Surveillance Center (NPDPSC), School of Medicine, Case Western Reserve University, Cleveland, OH; [5]Department of Neurology and Psychiatry, Case Western Reserve University School of Medicine/University Hospitals Cleveland Medical Center, Cleveland, OH; [6]National CJD Research and Surveillance Unit, Centre for Clinical Brain Sciences, University of Edinburgh, Edinburgh, UK; [7]Center for Neuropathology and Prion Research, Ludwig-Maximilians-Universität München, Munich, Germany; [8]Munich Cluster for Systems Neurology (SyNergy), Munich, Germany; [9]Department of Neuroscience, Istituto Superiore di Sanità, Rome, Italy

Additional supporting information can be found in the online version of this article.

Sporadic Creutzfeldt-Jakob disease (sCJD), the most prevalent human prion disease, remains a challenging diagnostic task for clinicians due to its rarity and substantial heterogeneity. It includes a broad spectrum of phenotypic variants, or "subtypes," characterized by distinctive clinical and histomolecular features. At the molecular level, sCJD subtypes are mainly defined by methionine (M) to valine (V) polymorphism at codon 129 of *PRNP*, the gene encoding the cellular prion protein (PrP^{C}), and the "type" of misfolded PrP (PrP^{Sc}) defined by the immunoblot profile of the fragments generated by proteinase-K digestion (ie, type 1, 21 kDa or type 2, 19 kDa, respectively).[1] Subtype classification and nomenclature are based on the combination of codon 129 genotype, and the PrP^{Sc} type (eg, MM1, MV1, VV2, VV1, etc.), with a few exceptions. They include the merging of MM1 and MV1 in the MM/MV1 subtype due to the lack of phenotypic differences, and the splitting of MM2 and MV2 groups into 2 distinct subtypes each, defined by distinctive histopathologic features. The former group was split into MM2-cortical (MM2C) and MM2-thalamic (MM2T), and the latter into MV2K and MV2C.[2] The consistent similarities across histopathologic features, PrP^{Sc} typing, and transmission properties between MM2C and MV2C, which is consistent with the preferential conversion of PrP^{C}-129 M into PrP^{Sc} (ie, PrP^{Sc}-129 M allotype) in MV2C, prompted the merging of MM2C and MV2C into a single subtype.[2–5] Thus, the current classification of sCJD includes the following 6 subtypes: MM/MV1, VV2, MV2K, MM/MV2C, MM2T, and VV1. Initially proposed in 1999,[6] this classification has received substantial biological confirmation and support for its generalizability, including the demonstration that 5 out of 6 subtypes behave as distinct prion strains upon serial experimental transmissions. Accordingly, they were named M1 (isolated from MM1 and MV1 inocula), V2 (VV2 and MV2K), M2C (MM2C), M2T (MM2T), and V1 (VV1).[7] Notably, subtypes linked to M1 and V2 prions account for most sCJD cases. Among the others, the MM/MV2C subtype has raised significant attention due to the relatively slow progression and early involvement limited to the cerebral cortex, resulting in a clinical phenotype that is challenging to recognize in vivo, often leading to delayed diagnosis.[8,9] Moreover, its high prevalence as a nondominant subtype in mixed sCJD phenotypes in which 2 subtypes coexist in the same patient,[3,10] and the very low transmission efficiency in experimental animal models,[7] make the MM/MV2C subtype of interest also from a neurobiological perspective. To date, the rarity of the MM/MV2C subtype has limited its comprehensive characterization. Nonetheless, aiming to improve the clinical recognition of such patients, subtype-specific diagnostic criteria have been recently proposed.[11] These criteria showed, preliminarily, a good accuracy in a small cohort (n = 9, all MM at codon 129) but lack confirmation in larger and external cohorts. Here, we performed a systematic analysis of clinical, histopathologic, and molecular features (PrP^{Sc}, genetics) in the largest sCJD MM/MV2C cohort reported to date and re-assessed the accuracy of the proposed diagnostic criteria.

Materials and Methods

Ethic Statement

The study was conducted according to the revised Declaration of Helsinki and Good Clinical Practice guidelines. All medical information was collected as part of national surveillance programs for prion diseases and approved by the local institutional review board for each country/participating center (CE-ISS 09/266, May 2009). All patients' data and samples were coded to protect their identities. Written informed consent was given by study participants or the next of kin.

Patient Selection and Classification

We included 56 patients who had a definite sCJD diagnosis, as determined by postmortem brain tissue studies according to molecular and histopathological consensus criteria.[2,12] Thirty-one patients were from the Neuropathology Laboratory at the Institute of Neurological Science of Bologna (ISNB), Italy, 15 from the National Prion Disease Pathology Surveillance Center (NPDPSC) of the United States, in Cleveland, Ohio, 6 from the Center for Neuropathology and Prion Research of the Ludwig-Maximilians-Universität, Munich, Germany, and 4 from the National Creutzfeldt-Jakob Disease Research and Surveillance Unit (NCJDRSU), University of Edinburgh, United Kingdom. All diagnoses were reviewed at ISNB. To this aim, histopathologic characterization in all cases and PrP^{Sc} typing in 45 of them were also carried out at ISNB. Moreover, the original Western blot analyses performed at NPDPSC in 11 cases were reviewed by 2 independent experts (authors P.P. and I.C.). We included both "pure" (MM/MV2C) and "mixed" (MM/MV2C + 1 and MV2C + 2K) histotypes. Specifically, we attributed the designation of MM/MV2C + 1 only to participants with a predominant type "2C" phenotype, in which the mean total amount of PrP^{Sc} type 2 (total type 2 "load"), expressed in percentage of total PrP^{Sc} signal on Western blot, after averaging all brain regions examined (see below), was higher than that of type 1 (ie, at least 51%).[3] In contrast, we based the definition of MV2C + 2 K on the presence of a predominant coarse/perivacuolar PrP accumulation at immunohistochemistry (ie, the hallmark of the MM/MV2C histotype) in all neocortices, striatum, and thalamus. Of note, 3 cases showing only PrP^{Sc} type 2 in all brain regions were classified as MM2C + 1 due to the finding of synaptic-type PrP deposits in the molecular layer of cerebellum (ie, hallmark of MM/MV1 histotype). This is because, when PrP^{Sc} type 1 is very focal or limited in amount,

histopathologic examination is more sensitive than PrP^{Sc} typing. According to the criteria above, 23 cases were classified as MM/MV2C (20 MM and 3 MV), 31 as MM/MV2C + 1 (23 MM and 8 MV), and 2 as MV2C + 2K (Supplementary Fig S1).

Molecular Genetic Analyses

To rule out pathogenic *PRNP* mutations and determine the codon 129 genotype, we performed PCR amplification and sequencing of genomic DNA, following a previously published protocol.[13]

Histopathologic Assessment

Standard routine histopathological staining was performed in all brains. A semiquantitative evaluation of gray matter spongiosis, astrogliosis, and neuronal loss was carried out by analyzing 8-micrometer-thick hematoxylin eosin-stained sections obtained from at least 10 brain regions (Supplementary Methods). The same experienced neuropathologist (author P.P.) rated spongiform change on a 0 to 4 scale (not detectable, mild, moderate, severe, and status spongiosus), as well as astrogliosis and neuronal loss on a 0 to 3 scale (not noticeable, mild, moderate, and severe). Then, a lesion profile for each patient was obtained by averaging the 3 scores.

PrP Immunohistochemistry

Immunohistochemistry for PrP was performed on formalin-fixed and paraffin-embedded blocks of the following areas: frontal and occipital neocortices, hippocampus, striatum, thalamus, periaqueductal gray, and cerebellum (see Supplementary Methods). PrP deposits were described according to the terminology proposed by a panel of experts in the field.[2]

Misfolded Prion Protein Typing

Preparation of brain homogenates and PrP^{Sc} typing by Western blot was performed according to established methods.[14,15] In all cases analyzed at ISBN (n = 45), we performed immunoblots in samples from the temporal, parietal, occipital lobes, and medial thalamus. To evaluate the regional variability of PrP^{Sc} typing in depth, we extended the analysis to 8 areas (frontal, temporal, parietal and occipital lobes, hippocampus, striatum, thalamus, and cerebellum) in a subgroup of 32 individuals. To assess the total type 2 load, Western blot signals were measured by densitometry using AIDA software (Image Data Analyzer version 4.15, Raytest, Isotopenmessgeraete GmbH, Straubenhardt, Germany).

Clinical Analysis

We reviewed the clinical chart for each patient's neurological symptoms and signs at the onset and during the disease course. We defined as "onset symptom(s)" the first neurological disturbance(s) complained by the patient or documented by neurological examination, and as "early symptoms" those reported in the first third of total disease duration in each patient. Moreover, we calculated the mean time of appearance of all reported symptoms/signs from disease onset, grouped according to the following categories: cerebellar, psychiatric, myoclonus, visual, pyramidal, parkinsonism, cognitive (mild impairment), dementia, non-myoclonic involuntary movements (ie, other dyskinesias), and akinetic mutism. Disease duration was calculated from the presentation of neurological signs to death. Patients with limited medical information (n = 5) were excluded from the clinical analysis.

Diagnostic Investigations

Cerebrospinal Fluid Analyses

Prion Real-Time Quaking-Induced Conversion. Prion real-time quaking-induced conversion (RT-QuIC) assay using CSF and full-length (residues 23–231, PQ-cerebrospinal fluid [CSF]) or truncated (residues 90–231, IQ-CSF) hamster recombinant prion protein as substrate was performed as previously described.[16–18]

Protein 14-3-3. Protein 14-3-3 in CSF was detected semiquantitatively by Western blot, as described.[19] Alternatively, we measured 14-3-3 gamma isoform using a commercially available enzyme-linked immunosorbent assay (ELISA) assay kit (Circulex 14–3-3 gamma ELISA kit, MBL, Woburn, MA) according to the manufacturer's instructions. For ELISA analyses, we considered "positive" 14-3-3 values greater than 23,400 AU/ml, according to our in-house cutoff.[20]

Magnetic Resonance Imaging. We reviewed all available cerebral magnetic resonance imaging (MRI) results, focusing on studies including fluid-attenuated inversion recovery (FLAIR) and diffusion-weighted imaging (DWI) sequences. Studies without FLAIR/DWI sequences were not analyzed further. Specifically, we searched for hyperintensities on FLAIR and/or DWI sequences in temporal, parietal and occipital cortices, striatum (caudate and putamen nuclei), thalamus, hippocampus, and insula. The time of MRI studies from the onset of symptoms was analyzed. According to current diagnostic criteria for sCJD,[21] we considered as "typical" findings the presence of hyperintensities on FLAIR and/or DWI in at least 2 cortical regions and/or the striatum.

Electroencephalography. Electroencephalography (EEG) recordings were reviewed, and abnormal traces were classified as follows: (a) diffuse nonspecific slowing, (b) paroxysmal discharges, and (c) periodic sharp-wave complexes (PSWCs).[22] When multiple EEG recordings were available for review, we assigned the highest degree of severity according to the following rule: PSWCs > paroxysmal discharges > slowing. We also collected the timing of each EEG recording (ie, time from onset of clinical symptoms).

Other Surrogate Biomarkers of Neurodegeneration

CSF total tau (t-tau) and neurofilament light chain (NfL) were measured by automated chemiluminescent enzyme immunoassay on the Lumipulse G600II platform (Fujirebio, Gent, Belgium), whereas plasma NfL was measured with the SiMOA NF-light

advantage kit on a SiMOA SR-X analyzer platform (Quanterix, Billerica, MA).

Results

Estimated Prevalence

In the neuropathologic ISNB cohort (2001–2024), including 594 consecutive brains from individuals with definite sCJD, MM/MV2C (both pure and mixed forms) was the fourth most prevalent histotype, accounting for 5.2% of cases.

Molecular Genetic Analyses

None of the participants carried pathogenic mutations in the *PRNP* open reading frame. Forty-three (76.8%) patients had the MM and 13 (23.2%) the MV genotype at codon 129. Of note, the relative frequency of the mixed histotype (see below) was higher in participants with 129MV than in those with the 129MM genotype (10/13, 76.9% vs 23/43, 53.4%, $p = 0.20$), although this difference was not statistically significant.

PrP^{Sc} Typing

The immunoblot profile of proteinase K-resistant PrP^{Sc} showed an unglycosylated fragment migrating at 19 kDa (type 2) in all participants (Fig 1). We detected only PrP^{Sc} type 2 in 27 cases (including all NPDPSC cases), whereas in 27 cases the predominant type 2 was associated with type 1 (ie, 2 > 1) in at least one analyzed area. Predominant type 2 was defined as a total PrP^{Sc} type 2 load > 51% calculated in immunoblot analyses of temporal, parietal, occipital cortices, and thalamus. When we examined the regional variability of PrP^{Sc} typing in 8 regions, instead of 4, the recognition of mixed histotypes did not improve. The cerebellum was the brain area where type 1 was more consistently detected (ie, 53.1% of cases showed exclusive or predominant type 1; Table 1). In 2 individuals carrying MV at *PRNP* codon 129, PrP^{Sc} type 2 was associated with a variable relative amount of a 20 kDa fragment ("intermediate" PrP^{Sc} type), most evident in the thalamus and striatum, whereas less represented in the neocortices. We found a slightly higher percentage of cases showing both PrP^{Sc} types 1 and 2 in patients carrying 129MV than in those MM (8/13, 61.5% vs 20/43, 46.5%), but the total type 2 load was comparable between groups (84 ± 12% vs 85 ± 16%).

As in other sCJD subtypes, monoglycosylated PrP^{Sc} was predominant in all MM/MV2C brains. However, as compared with typical MM/MV1, we found a relatively higher representation of the unglycosylated band and a proportional under-representation of the monoglycosylated isoform, resulting in a reduction of the ratio between glycosylated/unglycosylated PrP^{Sc} species in all areas analyzed (Supplementary Table S1).

Neuropathology

Spongiform change, characterized by large (diameter 15–20 μm) and confluent vacuoles, often organized in "grape-like" clusters (Fig 2), was widespread in the neocortex, being most pronounced in the temporal and occipital lobes. The thalamus and striatum were consistently affected, but usually less than the neocortex. In contrast, the hippocampus, midbrain, and cerebellum were typically spared or showed mild neuropathological changes in the cases with longer disease duration. The lesion profile was quite similar to that of the most common MM/MV1 subtype, except for greater cortical pathology and absence of significant spongiform change in the cerebellum. Accordingly, the mixed histotype MM/MV2C + 1 showed a significantly higher lesion severity score in the cerebellum than pure MM/MV2C. At the same time, MV2C + 2K had more pronounced pathology in both midbrain and

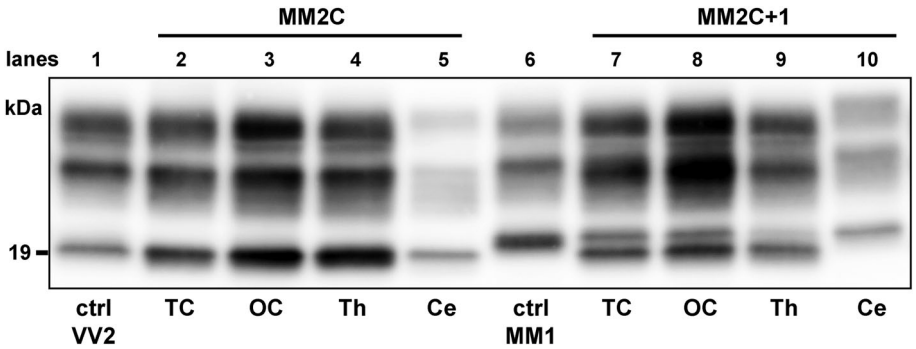

FIGURE 1: Regional immunoblot profiles of proteinase K-resistant PrP^{Sc} fragments in 2 representative sporadic Creutzfeldt-Jakob disease MM2C and MM2C + 1 cases. In pure MM2C (lanes 2–5), the unglycosylated PrP^{Sc} band migrates at 19 kDa (PrP^{Sc} type 2). In mixed MM2C + 1, a fragment migrating at 21 kDa (PrP^{Sc} type 1) is detected together with dominant PrP^{Sc} type 2 in neocortices (lanes 7–9), and alone in the cerebellum (lane 10). Of note, the diglycosylated/unglycosylated ratio was greater in the VV2 subtype (lane 1) than in MM2C (lanes 2–5). Immunoblot is probed with the mAb 3F4. ctrl = control; TC = temporal cortex, OC = occipital cortex, Th = thalamus; Ce = cerebellum.

TABLE 1. Relative PrP^{Sc} Type 1 and 2 Amounts and Regional Distribution in 8 Brain Regions in a Subgroup of 32 Patients

	FC (%)	TC (%)	PC (%)	OC (%)	Hipp (%)	Str (%)	Th (%)	Ce (%)
Type 2	19 (59.4)	22 (68.8)	19 (59.4)	19 (59.4)	15 (46.9)	16 (50.0)	19 (59.4)	13 (40.6)
Type 2 > 1	11 (34.4)	9 (28.1)	8 (25.0)	9 (28.1)	8 (25.0)	13 (40.6)	9 (28.1)	2 (6.3)
Type 1 = 2	1 (3.1)	1 (3.1)	3 (9.4)	1 (3.1)	5 (15.6)	1 (3.1)	2 (6.3)	0 (0.0)
Type 1 > 2	0 (0.0)	0 (0.0)	2 (6.3)	2 (6.3)	2 (6.3)	2 (6.3)	2 (6.3)	7 (21.9)
Type 1	1 (3.1)	0 (0.0)	0 (0.0)	1 (3.1)	2 (6.3)	0 (0.0)	0 (0.0)	10 (31.2)

The relative intensity of unglycosylated PrP^{Sc} peptides was evaluated by semiquantitative densitometry: when both type 1 and 2 were detected, isointensity was defined as a difference of signal intensity ≤ 5%, whereas a band was defined "predominant" when the difference was > 6%. FC = frontal cortex; TC = temporal cortex; PC = parietal cortex; OC = occipital cortex; Hipp = hippocampus; Str = striatum; Th = thalamus; Ce = cerebellum.

cerebellum than pure MM/MV2C. We found no significant differences in vacuoles type/distribution and the lesion profile of 129MM and 129MV cases (Supplementary Fig S2).

PrP immunochemistry revealed coarse deposits typically surrounding large vacuoles in the neocortices and striatum (ie, perivacuolar pattern), which is the hallmark of MM/MV2C histotype. All cases showed perivacuolar coarse PrP deposition in the neocortex, except for one, in which spongiform change was replaced by status spongiosus in the occipital cortex (Table 2). Instead of the perivacuolar pattern, scattered, patchy, coarse PrP were detected in the hippocampus, midbrain, where they mainly localized in the periaqueductal grey region, and to a lesser extent in the thalamus. In the cerebellum, immunoreactivity was confined to the molecular layer, except for the MV2C + 2K, showing kuru plaques and plaque-like deposits in the granular layer. The most frequent PrP deposition patterns in the molecular layer were (i) patchy coarse, often with focal distribution and no clear association with spongiform change, in pure MM/MV2C, and (ii) punctate synaptic usually co-localized with spongiosis in MM/MV2C + 1. In the latter group, synaptic deposits were also frequently detected in cortical regions and deep nuclei (Supplementary Table S2). The synaptic pattern was strongly associated with PrP^{Sc} type 1 load, particularly in the cerebellum (odds ratio = 41.5, 95% confidence interval [CI] = 5.3–325.4, $p < 0.001$). Next, we assessed the consistency between PrP^{Sc} type 1 detection and occurrence of synaptic PrP deposition in the cerebellar molecular layer in a subgroup of 30 cases with PrP^{Sc} typing in 8 brain areas and PrP immunohistochemistry available. All but one case (15/16, 93.8%) with detectable PrP^{Sc} type 1, either alone or mixed with type 2, showed synaptic PrP deposits as expected. Of the 14 cases with only PrP^{Sc} type 2 detectable in the cerebellum, 3 were negative at immunochemistry (21.4%), 10 showed only patchy/coarse deposits (71.4%), and 1 displayed both synaptic and patchy/coarse PrP deposits (7.1%). After excluding the immunohistochemistry-negative cases, the overall concordance between molecular PrP^{Sc} typing and immunohistochemistry was 92.6%.

Finally, in contrast with a previous report,[23] we did not find significant oligodendroglial PrP pathology in our cohort.

Remarkably, we were not able to detect any PrP immunoreactivity in the hippocampus (n = 26), striatum (n = 1), midbrain (n = 14), and cerebellum (n = 5) in a subgroup of pure cases.

Clinical Features

Among the 56 examined participants, 64.3% were females. The mean age at clinical onset was 64.5 ± 7.7 years (range = 47–82), and the mean disease duration was 16.0 ± 9.7 months (range = 4.5–61). Participants in the MM/MV2C + 1 group were older than those in pure MM/MV2C (65.7 ± 6.8 vs 60.9 ± 8.1 years, $p = 0.031$) and, although not statistically significant, showed a shorter total disease duration (14.3 ± 7.2 vs 19.2 ± 13.4 months).

Illness presentation was characterized by single or multiple domain mild cognitive impairment in most cases (Fig 3, Table 3); patients usually complained of forgetfulness and word-finding difficulty. Although poor cognitive performance was noted in all cases during the disease course, overt dementia was rare in the early disease stage. Cortical involvement was also documented by visual symptoms of central origin, including visual field loss, prosopagnosia, visual hallucinations, and visual agnosia in 35% to 40% of patients and occurring as an isolated presenting feature in 2 patients. Psychiatric symptoms and

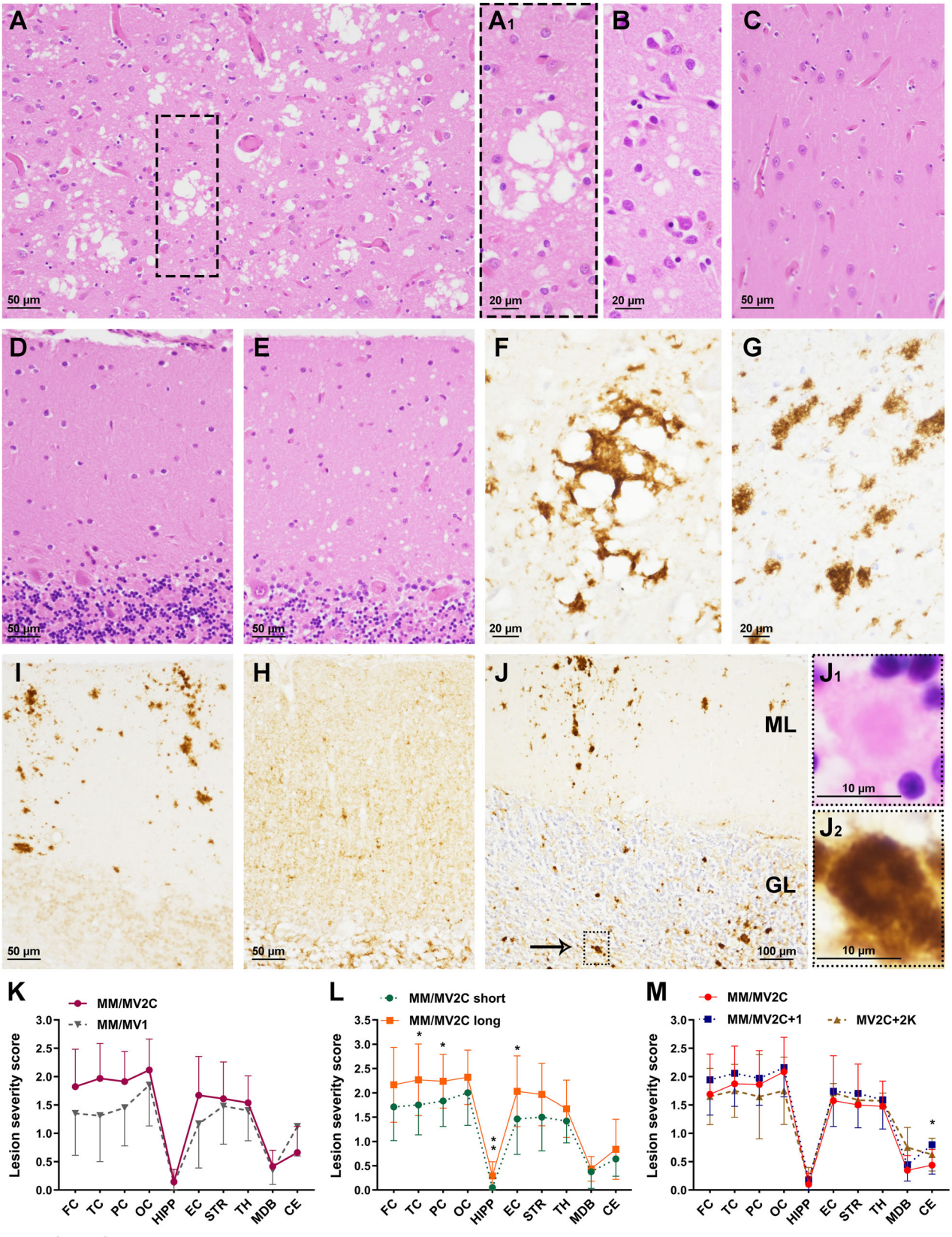

(Figure legend continues on next page.)

TABLE 2. Patterns of Prion Protein Deposition at Immunohistochemistry

	n	Coarse/PV	Coarse/patchy	Synaptic	Kuru plaques	Plaque-like
Frontal cortex	55	55 (100)	0 (0.0)	12 (21.8)	0 (0.0)	0 (0.0)
Occipital cortex	50	49 (98.0)	0 (0.0)	7 (14.0)	0 (0.0)	0 (0.0)
Hippocampus	48	6 (12.5)	13 (27.1)	4 (8.3)	0 (0.0)	0 (0.0)
Striatum	55	52 (94.5)	2 (3.6)	7 (12.7)	0 (0.0)	0 (0.0)
Thalamus	53	43 (81.1)	10 (18.9)	10 (18.9)	0 (0.0)	2 (3.8)
Periaqueductal gray	46	10 (21.7)	21 (45.6)	3 (6.5)	0 (0.0)	2 (4.3)
Cerebellum	53	0 (0.0)	36 (67.9)	25 (47.2)	2 (3.8)	2 (3.8)

Data are expressed as n (%). No immunoreactivity detectable: hippocampus, n = 26; striatum, n = 1; periaqueductal gray, n = 14, cerebellum, n = 5. PV = perivacuolar.

behavioral changes were commonly reported in the earliest disease stage. As the disease progressed, approximately 1 year after disease onset, patients developed parkinsonism (37%), myoclonus (61%), pyramidal signs (65%), and dementia (98%). Cerebellar symptoms/signs were reported in only 40% of cases, rarely in early stages, being more frequent and earlier in the MM/MV2C + 1 group than in pure MM/MV2C (Supplementary Table S3). Similarly, MM/MV2C + 1 patients developed dementia, non-myoclonic dyskinesias (eg, chorea and dystonia), and akinetic mutism earlier than pure MM/MV2C.

Diagnostic Investigations

CSF Analyses

Prion RT-QuIC. Prion-RT-QuIC was performed in 30 cases: PQ-CSF in 19, IQ-CSF in 26, and both protocols in 15 CSF. Overall, 21 of 30 (70.0%) CSFs tested positive, 7 were negative, and 2 were undetermined. IQ-CSF showed an increased sensitivity compared with PQ-CSF (in the subgroup tested by both assays, IQ-CSF 86.7% vs PQ-CSF 46.7%, $p = 0.05$). After histotype stratification, diagnostic sensitivity was higher in the mixed MM/MV2C + 1 group than in pure MM/MV2C (85.7% vs 53.3%).

Protein 14-3-3. CSF 14-3-3 protein was detected in 18 of 35 tested patients (51.4%), demonstrating a suboptimal performance. We found no difference between MM/MV2C and MM/MV2C + 1 groups (52.9% vs 47.1%). Patients with a positive 14-3-3 finding showed higher median CSF t-tau levels than those 14-3-3 negative (2,628 vs 1,075, $p = 0.0002$).

Magnetic Resonance Imaging. Brain MRI, including DWI and FLAIR sequences, demonstrated high diagnostic sensitivity, being positive in 97.1% of tested patients (33 of 34; Table 4). In most cases, high-intensity signals involved the neocortices of all lobes, showing a typical "cortical ribbon" pattern, whereas striatum and thalamus were less frequently affected (Fig 4). The involvement of deep grey nuclei and limbic areas, in particular the insular cortex, was more pronounced in MM/MV2C + 1 cases. However, because the mean time from clinical onset was longer for this group, we cannot definitely rule out that hyperintensity localization in these anatomic regions reflects a later disease stage.

FIGURE 2: Neuropathologic features of sporadic Creutzfeldt-Jakob disease MM/MV2C. (A) Spongiform change with large size, confluent vacuoles. (A_1, B) Comparison between large (A_1) and small (MM1 case, B) size vacuoles. (C) Sparing of the hippocampus and (D) cerebellar molecular layer in pure MM/MV2C. (E) Microvacuoles in the cerebellar molecular layer of an MM/MV2C + 1 case. (F) Coarse PrP deposits surrounding large vacuoles (perivacuolar pattern) in the neocortex, and (G) with scattered distribution in the thalamus. (I) Patchy coarse PrP accumulation in the molecular layer of the cerebellum. (H) Fine, synaptic PrP deposition in cerebellar molecular layer of an MM/MV2C + 1 case. (J) Representative findings in the cerebellum of MV2C + 2 K cases: patchy coarse PrP deposits in the molecular layer (ML), and kuru plaques/plaque-like deposits in the granule layer (GL) (J_1 and J_2 show details at higher magnification of kuru plaque). (K) Comparison between the lesion profile of subtypes MM/MV2C and MM/MV1. (L) Lesion profiles of MM/MV2C with long and short disease duration. (M) Comparison between lesion profiles of pure MM/MV2C, MM/MV2C + 1 and MV2C + 2 K. A to E, J_1 = Hematoxylin and eosin staining, F to J, J_2: PrP immunohistochemistry with the mAb 3F4. FC = frontal cortex, TC = temporal cortex, PC = parietal cortex, OC = occipital cortex, HIPP = hippocampus, EC = entorhinal cortex, STR = striatum, TH = thalamus, MDB = midbrain, CE = cerebellum, *$p \leq 0.05$.

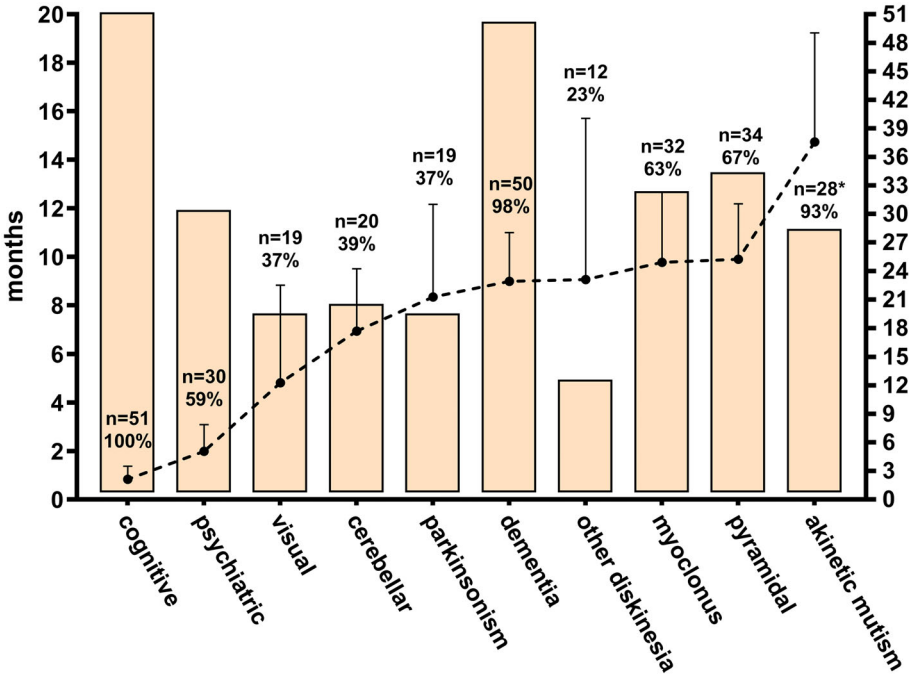

FIGURE 3: Clinical course of sporadic Creutzfeldt-Jakob disease MM/MV2C. The dashed line indicates the mean time of appearance (in months) from disease onset, whereas the bars represent the frequency for each group of symptoms/signs. *Since in a minority of clinical reports, the description of late symptoms was scanty or lacking, the number of patients indicated may not reliably represent the real frequency of akinetic mutism.

Electroencephalography. EEG recordings performed in 45 patients with a mean delay time from onset of 8.2 ± 5.7 months showed nonspecific diffuse slowing in 26 patients (57.8%). Typical PSWCs were identified in 13 patients (28.9%). Remarkably, 11 of them (84.6%) belonged to the MM/MV2C + 1 group, 1 to MV2C + 2K, and only 1 to MM/MV2C. Paroxysmal activity was identified in 4 cases (8.9%), whereas EEG was unremarkable in 2 (4.4%).

TABLE 3. Clinical Symptoms at Onset and During Early Stages in 51 Patients

Symptoms at onset, n	%	Early symptoms, n[a]	%
Loss of intellectual abilities,[b] 24	47.1	Loss of intellectual abilities/dementia, 35	68.6
Memory loss, 18	35.3	Memory loss, 23	45.1
Behavioral change/psychiatric,[c] 13	25.5	Behavioral change/psychiatric, 18	35.3
Confusion/disorientation, 8	15.7	Confusion/disorientation, 14	27.5
Gait unsteadiness, 7	13.7	Aphasia, 14	27.5
Aphasia, 6	11.8	Gait unsteadiness, 11	21.6
Visual misperception, hallucination, or agnosia, 5	9.8	Visual misperception, hallucination, or agnosia, 10	19.6
Vision loss, 3	5.9	Involuntary movements, 7	13.7
Involuntary movements,[d] 2	3.9	Parkinsonism, 7	13.7
Parkinsonism, 2	3.9	Vision loss, 5	9.8

[a]Early symptoms were those manifesting in the first third of total disease duration calculated for each patient (only those occurring in at least 5 patients were reported).
[b]Loss of intellectual abilities includes attention deficit, slow thinking, and multiple-domain cognitive dysfunction.
[c]Behavioral changes include one or more of the following: apathy, abulia, psychomotor agitation, aggressiveness, irritability, and oddness.
[d]Involuntary movements include chorea, athetosis, dystonia, and myoclonus.

TABLE 4. Magnetic Resonance Imaging Findings.

	All*	MM/MV2C	MM/MV2C + 1	MV2C + 2 K
N	34	16	17	1
Positive examination (typical)[a]	33 (97.1)	16 (100)	16 (94.4)	1 (100)
Topographic distribution of hyperintensities[b]				
Striatum	12 (36.4)	3 (18.7)	9 (56.2)	0 (0.0)
Neocortices[#]	31 (93.9)	15 (93.7)	15 (93.7)	1 (100)
Temporal	26 (78.8)	13 (91.3)	13 (91.3)	0 (0.0)
Parietal	29 (87.9)	15 (93.7)	14 (87.5)	1 (100)
Occipital	24 (72.7)	10 (62.5)	13 (91.3)	1 (100)
Thalamus	6 (18.2)	2 (12.5)	4 (25.0)	0 (0.0)
Limbic	7 (21.2)	2 (12.5)	5 (31.2)	0 (0.0)
Hippocampus	1 (3.0)	0 (0.0)	1 (6.3)	0 (0.0)
Insula	7 (21.2)	2 (12.5)	5 (31.2)	0 (0.0)
Timing (mo)	6.4 ± 3.9	5.3 ± 2.6	7.5 ± 4.8	3.00

Only the examinations including DWI and/or FLAIR sequences were included. Data are expressed as n (%).
[a]Positive examination was defined according with revised diagnostic criteria for sporadic Creutzfeldt-Jakob disease.
[b]Frequencies were calculated only for typical cases.

Other Surrogate Biomarkers of Neurodegeneration

As in other prion disease subtypes, t-tau and NfL in both CSF and plasma, were increased in MM/MV2C. After setting a validated cutoff discriminative for sCJD at t-tau > 1,250 pg/ml,[19] we correctly identified 17 of 30 cases (56.7%), confirming, as for 14-3-3 protein, a suboptimal performance of t-tau. Although the sample size was limited, all surrogate biomarker levels (CSF t-tau, CSF NfL, and plasma NfL) were higher in pure

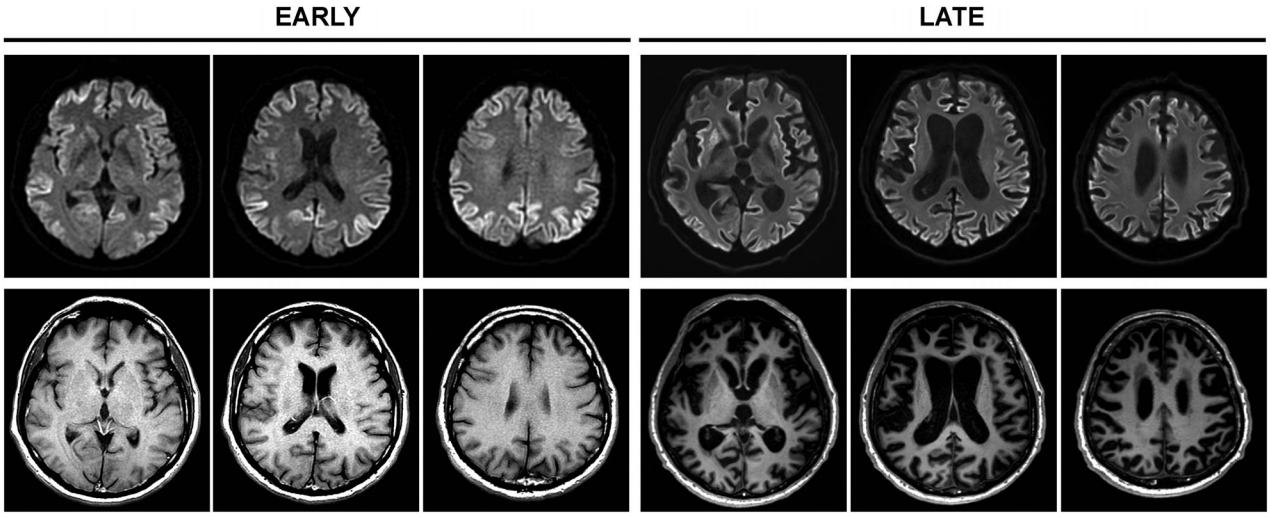

FIGURE 4: Representative Magnetic Resonance Imaging findings in a patient with pure MM2C in early and late disease stages. The upper micrographs (DWI sequences) show pronounced cortical hyperintense ribboning in the early stage. In contrast, hyperintensity of the caudate and putamen nuclei is most evident in the late stage, together with an overall reduction of cortical high signal. The boxes on the bottom (T1 sequences) display a marked progression of cortical atrophy from early to late stage.

MM/MV2C than in MM/MV2C + 1 (Supplementary Fig S3).

Application of Clinical Diagnostic Criteria to MM/MV2C

We retrospectively applied the 2019 diagnostic criteria for sCJD to 30 patients (ie, MM2C, n = 11; MM2C + 1, n = 14; MV2C, n = 1; MV2C + 1, n = 3; and MV2C + 2 K, n = 1) with a comprehensive clinical assessment. Of these 28 (93.3%) were classified as "probable," 1 as "possible" (3.3%), and 1 as non-sCJD (3.3%). The latter participant did not fulfill the clinical (symptoms) criterion but showed typical DW-MRI cortical hyperintensities. We also evaluated the application of criteria at the time of diagnostic work-up (mean 6.7 ± 4.2 months): notably, 13 of 30 patients (43.3%) did not fulfill clinical criteria (ie, they cannot be diagnosed to have a "probable" disease, despite testing positive by DW-MRI). Therefore, prion RT-QuIC is crucial for reaching an accurate diagnosis in the early stage when clinical symptoms are often limited to cognitive impairment. Then, we applied the new criteria specific to sCJD MM2C proposed by Hamaguchi and colleagues (Supplementary Table S4): 18 cases met the criteria for "probable" (60%), and 6 for "possible" (20%) CJD, whereas 6 did not fulfill the criteria (20%). Because MM homozygosity at *PRNP* codon 129 is essential in these criteria we repeated the analysis in 25 subjects carrying 129MM: "probable" (72%) and "possible" (24%) cases were correctly recognized, limiting uncorrected diagnoses to 1 (4%). Finally, we restricted the analysis to pure MM2C cases (n = 11): all met at least the criteria for possible diagnosis: 9 cases (81.8%) were diagnosed with "probable," and 2 with "possible" (18.2%) MM2C. These results are overall consistent with previously reported criteria performance.[11]

Discussion

To further contribute to the understanding of sCJD clinical and histopathological heterogeneity and its molecular basis, here, we present the results of a comprehensive study on the largest MM/MV2C cohort reported to date. As the main results, we provide a refined characterization of the clinical and laboratory features that distinguish the MM/MV2C phenotype from the typical prevalent MM/MV1 subtype (ie, the clinical paradigm of sCJD), along with a critical revision of previously proposed MM2C-specific diagnostic criteria for the early identification of this subtype in clinical practice.

In our large cohort of sCJD-affected brains, MM/MV2C was the fourth most common subtype, accounting for approximately 5% of cases, including both "pure" (ie, MM/MV2C) and "mixed" forms in which MM2C represents the dominant phenotype (ie, MM/MV2C + 1 and MV2C + 2K). In line with previous studies in smaller cohorts,[8,9,11] we show that the clinical phenotype of MM/MV2C is primarily characterized by early cognitive decline and a disease progression which is significantly slower than in typical MM/MV1. Progressive cognitive decline in the absence of focal neurological signs raises the differential diagnosis with other neurodegenerative dementias, in particular Alzheimer's disease, dementia with Lewy bodies, and frontotemporal dementia. Besides cognitive impairment affecting different domains, the high frequency of behavioral/psychiatric and visual symptoms also reflects the primary cortical involvement, with the latter occurring in isolation at onset in a few cases,[24,25] featuring the so-called Heidenhain variant.

In contrast to typical MM/MV1, motor signs, comprising pyramidal and extrapyramidal signs, myoclonus, and other involuntary movements, usually appear late in the disease course, between 9 and 12 months after disease onset. Nevertheless, the finding of extrapyramidal signs at clinical onset in 3.9% of participants in our cohort, confirms that MM/MV2C can also occasionally challenge the diagnosis in front of an atypical parkinsonian syndrome.[26]

The consistent number of participants enabled us to demonstrate that the coexistence of PrP^{Sc} type 1 (despite the dominant type 2) significantly affects the clinical phenotype in mixed MM/MV2C + 1. Indeed, we found a shorter total disease duration, earlier progression to akinetic mutism and a higher prevalence of cerebellar signs in these "mixed" cases. Accordingly, we observed more severe pathological changes in the cerebellum in MM/MV2C + 1 than in pure MM/MV2C. Because the cerebellum is usually spared or only mildly affected in MM/MV2C, the prevalence of reported cerebellar signs in patients with the "pure" phenotype might be even overestimated, with features such as wide-based gait and unsteady walking caused by cortical rather than cerebellar dysfunction.

Because the early clinical phenotype of MM/MV2C often does not fulfil the features required by current diagnostic criteria for "possible" CJD, clinical awareness and diagnostic investigations are crucial for the accurate identification of this subtype. Our results confirm that DW-MRI is the most sensitive diagnostic test, demonstrating cortical hyperintensities in 94% of cases. High signal of striatum and thalamus is less common, especially in pure MM/MV2C. We also show that prion RT-QuIC is the most informative CSF biomarker (pooled sensitivity, 70%), with the IQ-CSF protocol showing a significantly higher sensitivity than PQ-CSF (87% vs 47%). Therefore, clinicians should be aware of the protocol used for

RT-QuIC analyses in suspected MM/MV2C cases, particularly when the test returns a negative result. Notably, we demonstrated a good sensitivity of the RT-QuIC (IQ-CSF) assay in MM/MV2C, although it was lower than in MM/MV1, VV2, and MV2K subtypes. Our results are in line with those from previous studies reporting 71% to 78% sensitivity of IQ-CSF protocol in this subtype.[18,27] The 14-3-3 protein and elevated t-tau levels in CSF had suboptimal sensitivity, being positive in only about half of the patients. EEG showed PSWCs in 29% of patients (a prevalence lower than previously reported),[28] mostly belonging to the MM/MV2C + 1 group, whereas they were exceedingly rare in patients with pure MM/MV2C.

Given the "atypical" phenotypic features, Hamaguchi et al have recently proposed subtype-specific criteria for the pure MM2C subtype aimed at improving clinical diagnosis. However, these criteria do not fully consider the molecular complexity within this subtype, given that this phenotype may also occur in "mixed" forms, especially MM/MV2C + 1, and in subjects carrying MV at codon 129. In this regard, we here confirmed the consistent histopathologic and molecular PrP^{Sc} features between 129MM and 129MV carriers, justifying the merging of MM2C and MV2C into one MM/MV2C subtype. In our cohort, 23% of cases were 129MV, suggesting that the criteria should be extended to include the 129MV genotype for accurate classification. Moreover, according to the Hamaguchi criteria, a "probable" MM2C diagnosis allows at most one of the following 4 clinical features within 6 months post-onset: (A) myoclonus, (B) pyramidal/extrapyramidal signs, (C) cerebellar ataxia or visual impairment, and (D) akinetic mutism. We found that 9 participants presented 2 or 3 of these clinical features in a subgroup of 30 patients with MM/MV2C with detailed clinical information comprising both MM/MV2C and MM/MV2C + 1 participants. The higher prevalence and earlier appearance of cerebellar signs, visual impairment, and myoclonus in MM/MV2C + 1 cases compared to pure MM/MV2C (see Table 4) largely explain the discrepancy with the series reported by Hamaguchi et al, underscoring the greater accuracy of these criteria for the pure forms.

The results from the study of PrP^{Sc} glycoforms deserve a separate comment. Here, we demonstrated a lower PrP^{Sc} glycosylated/unglycosylated isoform ratio in MM/MV2C compared with typical MM/MV1. This finding further supports previous evidence indicating an association between PrP^{Sc} glycosylation and prion replication and transmission efficiency.[29,30] Accordingly, CJD forms associated with the most abundant glycosylated PrP^{Sc} (ie, variants CJD and sCJD VV2) exhibit the highest transmission efficiency.[31] In contrast, the MM2C subtype showed a low propagation efficiency, being successfully transmitted (although with a reduced attack rate and with a long incubation time) only in transgenic mice overexpressing human PrP^{C} or expressing bank vole PrP,[32–34] but not in knock-in murine lines expressing human PrP^{C} at normal levels (ie, MM2C is the only sCJD subtype that does not transmit to these mice).[7]

Another relevant point worth discussing is the high prevalence of mixed forms in our cohort (57.1% of all cases), with MM/MV2C + 1 being the most frequent. Among them, we described, for the first time, the MV2C + 2K phenotype, characterized by "2C" dominance over "2K." This finding is consistent with the notion that MM/MV2C is the subtype that most frequently co-exists with other sCJD subtypes,[3] although it usually represents the non-dominant subtype.

The pathogenic mechanisms driving the co-existence of prion strains are not fully understood. It has been hypothesized that prion strains exist in a dynamic mixture of a predominant strain and minor substrains,[35] and that different individual genetic factors and pathogenic mechanisms (eg, prion interference) are responsible for the selection of one strain over others. In our scenario, prion strain interference would explain the development of the most prevalent MM/MV1 + 2C phenotype well.[36] Because prion strains compete with each other converting PrP^{C}, those with faster/more efficient replication (ie, M1) could interfere with the slower ones (ie, M2C), eventually favoring MM/MV1 dominancy over MM/MV2C. However, prion strain interference does not explain the mixed phenotypes described here, characterized by the dominant MM/MV2C subtype. Based on current knowledge of human prion disease, we suggest 2 hypotheses. The first considers a different timing between the selection and replication of the 2 PrP^{Sc} conformers. Accordingly, M2C prions would be initially selected, replicated, and spread throughout the brain, followed by the M1 prions in the late disease course, when M2C prions are already diffuse in the brain, distributing preferentially in brain regions spared by MM/MV2C, such as the cerebellum. This hypothesis would also be compatible with an exogenous source of prions in a mixture in which one PrP^{Sc} conformer is highly prevalent, allowing for earlier replication. The second hypothesis postulates that region-specific, genetically driven tissue characteristics, such as the PrP^{C} glycosylation state, may drive the local emergence of a specific strain over another.[37,38] For example, in a subgroup of 129MM or MV subjects, individual PrP^{C} glycosylation state (eg, abundance of unglycosylated PrP^{C} species and/or sialylation profile) could be responsible for a more diffuse selection and diffusion of M2C over M1 prions.

The main strength of this study is the significant number of cases included (the largest reported to date) and the comprehensive clinical, pathological, and molecular characterization. The main limitation is the heterogeneity of the centers where clinical evaluations were done, which could have impacted the internal consistency. However, this clinical heterogeneity well reproduces the real-life clinical setting where patients underwent neurological evaluations in different centers, often with limited expertise on prion disease.

In summary, the MM/MV2C is a rare subtype of sCJD accounting for approximately 5% of all cases. It is clinically distinct from the typical disease phenotype (MM/MV1) because of the presentation with slowly progressive cognitive decline without associated neurological signs, and a relatively long disease duration. The histomolecular heterogeneity within this subtype, mainly determined by the high prevalence of mixed forms, accounts for the clinical heterogeneity and variable sensitivity of diagnostic investigations. Overall, brain DW-MRI is the most sensitive diagnostic test, followed by CSF prion RT-QuIC, whereas other tests show suboptimal sensitivity. Awareness of the existence of a sCJD subtype presenting with isolated cognitive impairment not necessarily associated with rapid progression can lead to an early clinical diagnosis due to the accuracy of diagnostic investigation (ie, DW-MRI, CSF prion RT-QuIC assay, and codon 129 genotyping).

Acknowledgment

The authors wish to thank the patients, their families, and the numerous Italian neurologists who provided clinical information. We are also in debt to Barbara Polischi, MSc, for her valuable technical assistance. All UK human tissue samples examined in this study were provided by the National CJD Research and Surveillance Unit (NCJDRSU), which is part of the MRC Edinburgh Brain and Tissue Bank (Edinburgh Brain Bank 16-ES0084). Brain tissues of German cases were provided by NBM (Neurobiobank Munich). We would also like to thank the staff of the National Prion Disease Pathology Surveillance Center, who helped with many of the US cases included in the study. The study was supported by the grant "Ricerca Corrente" funded by the Italian Ministry of Health, and the #NextGenerationEU (NGEU), funded by the Ministry of University and Research (MUR), National Recovery and Resilience Plan (NRRP), project MNESYS (PE0000006) to S.B. and P.P., the Centers for Disease Control and Prevent (1NU38CK000486 grant) to B.S.A, and National Institutes of Health (NIH) K99/R00 AG068359 grants to I.C. The National CJD Research and Surveillance Unit is funded by the United Kingdom's Department of Health and Social Care Policy Research Programme and the Government of Scotland (PR-ST-0614-00008_18). The National Italian Registry of Creutzfeldt-Jakob diseases and related syndromes was funded by the Istituto Superiore di Sanità. Open access funding provided by BIBLIOSAN.

Potential Conflicts of Interest

Nothing to report.

Data availability

The data that support the findings of this study are available from the corresponding author, upon reasonable request.

Author Contributions

Simone Baiardi: Writing – review and editing; writing – original draft; formal analysis; validation; investigation. **Claudia Marina Vargiu:** Formal analysis; writing – review and editing; methodology. **Brian S. Appleby:** Writing – review and editing; formal analysis. **Marcelo Barria:** Writing – review and editing; formal analysis. **Giuseppe Mario Bentivenga:** Writing – review and editing; formal analysis; investigation. **Ignazio Calì:** Writing – review and editing; investigation. **Benedetta Carlà:** Writing – review and editing; formal analysis; methodology. **Mark Cohen:** Writing – review and editing; formal analysis; investigation. **Armin Giese:** Writing – review and editing; formal analysis; investigation. **Jochen Herms:** Writing – review and editing; formal analysis; investigation. **Aino-Minerva Kortelainen:** Writing – review and editing; formal analysis; investigation. **Anna Ladogana:** Writing – review and editing; formal analysis; data curation. **Angela Mammana:** Writing – review and editing; formal analysis; methodology. **Diane Ritchie:** Writing – review and editing; formal analysis. **Otto Windl:** Writing – review and editing; formal analysis. **Sabina Capellari:** Writing – review and editing; formal analysis; supervision. **Piero Parchi:** Writing – review and editing; conceptualization; writing – original draft; methodology; supervision; resources; data curation; validation; funding acquisition; formal analysis.

References

1. Parchi P, Castellani R, Capellari S, et al. Molecular basis of phenotypic variability in sporadc creudeldt-jakob disease. Ann Neurol 1996;39:767–778. https://doi.org/10.1002/ana.410390613.

2. Parchi P, de Boni L, Saverioni D, et al. Consensus classification of human prion disease histotypes allows reliable identification of

molecular subtypes: an inter-rater study among surveillance centres in Europe and USA. Acta Neuropathol 2012;124:517–529. https://doi.org/10.1007/s00401-012-1002-8.

3. Parchi P, Strammiello R, Notari S, et al. Incidence and spectrum of sporadic Creutzfeldt-Jakob disease variants with mixed phenotype and co-occurrence of PrPSc types: an updated classification. Acta Neuropathol 2009;118:659–671. https://doi.org/10.1007/s00401-009-0585-1.

4. Kobayashi A, Iwasaki Y, Otsuka H, et al. Deciphering the pathogenesis of sporadic Creutzfeldt-Jakob disease with codon 129 M/V and type 2 abnormal prion protein. Acta Neuropathol Commun 2013;1:74. https://doi.org/10.1186/2051-5960-1-74.

5. Nemani SK, Xiao X, Cali I, et al. A novel mechanism of phenotypic heterogeneity in Creutzfeldt-Jakob disease. Acta Neuropathol Commun 2020;8:85. https://doi.org/10.1186/s40478-020-00966-x.

6. Parchi P, Giese A, Capellari S, et al. Classification of sporadic Creutzfeldt-Jakob disease based on molecular and phenotypic analysis of 300 subjects. Ann Neurol 1999;46:224–233.

7. Bishop MT, Will RG, Manson JC. Defining sporadic Creutzfeldt-Jakob disease strains and their transmission properties. Proc Natl Acad Sci USA 2010;107:12005–12010. https://doi.org/10.1073/pnas.1004688107.

8. Hamaguchi T, Kitamoto T, Sato T, et al. Clinical diagnosis of MM2-type sporadic Creutzfeldt-Jakob disease. Neurology 2005;64:643–648. https://doi.org/10.1212/01.WNL.0000151847.57956.FA.

9. Krasnianski A, Meissner B, Schulz-Schaeffer W, et al. Clinical features and diagnosis of the MM2 cortical subtype of sporadic Creutzfeldt-Jakob disease. Arch Neurol 2006;63:876–880. https://doi.org/10.1001/archneur.63.6.876.

10. Cali I, Castellani R, Alshekhlee A, et al. Co-existence of scrapie prion protein types 1 and 2 in sporadic Creutzfeldt-Jakob disease: its effect on the phenotype and prion-type characteristics. Brain 2009;132:2643–2658. https://doi.org/10.1093/brain/awp196.

11. Hamaguchi T, Sanjo N, Ae R, et al. MM2-type sporadic Creutzfeldt-Jakob disease: new diagnostic criteria for MM2-cortical type. J Neurol Neurosurg Psychiatry 2020;91:1158–1165. https://doi.org/10.1136/jnnp-2020-323231.

12. Parchi P, Notari S, Weber P, et al. Inter-laboratory assessment of PrPSc typing in creutzfeldt-jakob disease: a Western blot study within the NeuroPrion consortium. Brain Pathol 2009;19:384–391. https://doi.org/10.1111/j.1750-3639.2008.00187.x.

13. Baiardi S, Rossi M, Mammana A, et al. Phenotypic diversity of genetic Creutzfeldt-Jakob disease: a histo-molecular-based classification. Acta Neuropathol 2021;142:707–728. https://doi.org/10.1007/s00401-021-02350-y.

14. Notari S, Capellari S, Langeveld J, et al. A refined method for molecular typing reveals that co-occurrence of PrP(Sc) types in Creutzfeldt-Jakob disease is not the rule. Lab Investig 2007;87:1103–1112. https://doi.org/10.1038/labinvest.3700676.

15. Rossi M, Saverioni D, Di Bari M, et al. Atypical Creutzfeldt-Jakob disease with PrP-amyloid plaques in white matter: molecular characterization and transmission to bank voles show the M1 strain signature. Acta Neuropathol Commun 2017;5:87. https://doi.org/10.1186/s40478-017-0496-7.

16. McGuire LI, Poleggi A, Poggiolini I, et al. Cerebrospinal fluid real-time quaking-induced conversion is a robust and reliable test for sporadic creutzfeldt-jakob disease: an international study. Ann Neurol 2016;80:160–165. https://doi.org/10.1002/ana.24679.

17. Franceschini A, Baiardi S, Hughson AG, et al. High diagnostic value of second generation CSF RT-QuIC across the wide spectrum of CJD prions. Sci Rep 2017;7:10655. https://doi.org/10.1038/s41598-017-10922-w.

18. Foutz A, Appleby BS, Hamlin C, et al. Diagnostic and prognostic value of human prion detection in cerebrospinal fluid. Ann Neurol 2017;81:79–92. https://doi.org/10.1002/ana.24833.

19. Lattanzio F, Abu-Rumeileh S, Franceschini A, et al. Prion-specific and surrogate CSF biomarkers in Creutzfeldt-Jakob disease: diagnostic accuracy in relation to molecular subtypes and analysis of neuropathological correlates of p-tau and Aβ42 levels. Acta Neuropathol 2017;133:559–578. https://doi.org/10.1007/s00401-017-1683-0.

20. Abu-Rumeileh S, Baiardi S, Polischi B, et al. Diagnostic value of surrogate CSF biomarkers for Creutzfeldt-Jakob disease in the era of RT-QuIC. J Neurol 2019;266:3136–3143. https://doi.org/10.1007/s00415-019-09537-0.

21. Zerr I, Kallenberg K, Summers DM, et al. Updated clinical diagnostic criteria for sporadic Creutzfeldt-Jakob disease. Brain 2009;132:2659–2668. https://doi.org/10.1093/brain/awp191.

22. Wieser HG, Schindler K, Zumsteg D. EEG in Creutzfeldt-Jakob disease. Clin Neurophysiol 2006;117:935–951. https://doi.org/10.1016/j.clinph.2005.12.007.

23. Gelpi E, Klotz S, Vidal-Robau N, et al. Histotype-dependent Oligodendroglial PrP pathology in sporadic CJD: a frequent feature of the M2C "strain". Viruses 2021;13:1796. https://doi.org/10.3390/v13091796.

24. Nozaki I, Hamaguchi T, Noguchi-Shinohara M, et al. The MM2-cortical form of sporadic Creutzfeldt-Jakob disease presenting with visual disturbance. Neurology 2006;67:531–533. https://doi.org/10.1212/01.wnl.0000228224.35678.60.

25. Baiardi S, Capellari S, Ladogana A, et al. Revisiting the Heidenhain variant of Creutzfeldt-Jakob disease: evidence for prion type variability influencing clinical course and laboratory findings. J Alzheimer's Dis 2016;50:465–476. https://doi.org/10.3233/JAD-150668.

26. Petrovic IN, Martin-Bastida A, Massey L, et al. MM2 subtype of sporadic Creutzfeldt-Jakob disease may underlie the clinical presentation of progressive supranuclear palsy. J Neurol 2013;260:1031–1036. https://doi.org/10.1007/s00415-012-6752-7.

27. Rhoads DD, Wrona A, Foutz A, et al. Diagnosis of prion diseases by RT-QuIC results in improved surveillance. Neurology 2020;95:e1017–e1026. https://doi.org/10.1212/WNL.0000000000010086.

28. Matsubayashi T, Akaza M, Hayashi Y, et al. Focal sharp waves are a specific early-stage marker of the MM2-cortical form of sporadic Creutzfeldt-Jakob disease. Prion 2020;14:207–213. https://doi.org/10.1080/19336896.2020.1803516.

29. Baskakov IV, Katorcha E, Makarava N. Prion strain-specific structure and pathology: a view from the perspective of glycobiology. Viruses 2018;10:723. https://doi.org/10.3390/v10120723.

30. Aguilar-Calvo P, Callender JA, Sigurdson CJ. Short and sweet: how glycans impact prion conversion, cofactor interactions, and cross-species transmission. PLoS Pathog 2021;17:e1009123. https://doi.org/10.1371/journal.ppat.1009123.

31. Rossi M, Baiardi S, Parchi P. Understanding prion strains: evidence from studies of the disease forms affecting humans. Viruses 2019;11:309. https://doi.org/10.3390/v11040309.

32. Jaumain E, Quadrio I, Herzog L, et al. Absence of evidence for a causal link between bovine spongiform encephalopathy strain variant L-BSE and known forms of sporadic Creutzfeldt-Jakob disease in human PrP transgenic mice. J Virol 2016;90:10867–10874. https://doi.org/10.1128/JVI.01383-16.

33. Korth C, Kaneko K, Groth D, et al. Abbreviated incubation times for human prions in mice expressing a chimeric mouse-human prion protein transgene. Proc Natl Acad Sci USA 2003;100:4784–4789. https://doi.org/10.1073/pnas.2627989100.

34. Kobayashi A, Matsuura Y, Takeuchi A, et al. A domain responsible for spontaneous conversion of bank vole prion protein. Brain Pathol 2019;29:155–163. https://doi.org/10.1111/bpa.12638.

35. Collinge J, Clarke AR. A general model of prion strains and their pathogenicity. Science 2007;318:930–936. https://doi.org/10.1126/science.1138718.

36. Haldiman T, Kim C, Cohen Y, et al. Co-existence of distinct prion types enables conformational evolution of human PrPSc by competitive selection. J Biol Chem 2013;288:29846–29861. https://doi.org/10.1074/jbc.M113.500108.

37. Burke CM, Walsh DJ, Mark KMK, et al. Cofactor and glycosylation preferences for in vitro prion conversion are predominantly determined by strain conformation. PLoS Pathog 2020;16:e1008495. https://doi.org/10.1371/journal.ppat.1008495.

38. Makarava N, Chang JC-Y, Molesworth K, Baskakov IV. Posttranslational modifications define course of prion strain adaptation and disease phenotype. J Clin Invest 2020;130:4382–4395. https://doi.org/10.1172/JCI138677.